Available online at www.sciencedirect.com
ScienceDirect
Polymer 48 (2007) 2729–2736
polymer
www.elsevier.com/locate/polymer

Preparation of poly(ethylene terephthalate) nonwoven fabric from endless microfibers obtained by CO_2 laser-thinning method

Akihiro Suzuki*, Mahomi Kishi

Interdisciplinary Graduate of School of Medicine and Engineering, University of Yamanashi, Takeda-4, Kofu 400-8511, Japan

Received 4 November 2006; received in revised form 2 March 2007; accepted 10 March 2007
Available online 14 March 2007

Abstract

Poly(ethylene terephthalate) (PET) nonwoven fabric was prepared from microfibers obtained by using a carbon dioxide laser-thinning method. The PET nonwoven fabric obtained was made of the endless mircofibers with a uniform diameter without droplets. The fiber diameter can be varied by controlling airflow rate into the air jet and supplying speed of an original fiber into a laser-irradiating point. The fiber diameter decreased, and its birefringence increased as the airflow rate increased and the supplying speed decreased. When the microfiber prepared by irradiating the laser operated at a power density of 4.8 W cm^{-2} to the original fiber supplied at $S_s = 0.15$ m min^{-1} was dragged at an airflow rate of 30 L min^{-1}, the thinnest microfiber with a diameter of 3.6 μm was obtained.

Keywords: Poly(ethylene terephthalate); Nonwoven fabric; Laser thinning

1. Introduction

Nonwoven fabrics are industrially produced by a meltblowing [1–3], spunbonding [4–6] and flashspinning, and the nonwoven fabrics made of nanofibers are obtained by an electrospinning [7–10]. The spunbonding is the integrated process combining fiber spinning, web formation, and bonding. The spunbonded fabrics are made of the continuous filament with a diameter of about 10 μm. The meltblown and flashspun fabrics are composed of staple fibers with an inhomogeneous diameter in the range of 1–10 μm, and the meltblown fabrics included droplets sometimes.

The nonwoven fabrics are exploited in a large number of applications such as membrane [11–13], reinforcing fibers [14], biomedical devices [15], and scaffold for tissue engineering [16–20]. The nonwoven fabrics made of the microfiber and nanofiber are most useful in the tissue engineering because of large surface area per unit mass and very small pore size. However, the flashspun and the electrospun fabrics will not be able to implant in a living body because the solvents harmful to the living body are used in their producing processes. Although the solvent contained in the electrospun fabric evaporates in the electric field formed between the capillary tube and the metallic collector, it is difficult to completely remove the solvent.

Microfibers are very valuable from the viewpoint of industrial and medical materials and are now manufactured with highly skilled techniques, such as conjugate spinning and islands-in-a-sea fiber spinning. On the other hand, a carbon dioxide (CO_2) laser-thinning method developed by us could easily produce the microfiber without using a highly complex spinneret such as the conjugate spinning [21]. The CO_2 laser-thinning method was previously applied to poly(ethylene terephthalate) (PET) [22], nylon 6 [23], isotactic polypropylene [24], nylon 66 [25], and poly(L-lactic acid) (PLLA) [26], to produce their microfibers, and then their microfibers with a diameter of about 2 μm were obtained. The CO_2 laser-thinning apparatus preparing the microfiber could be also produced the nonwoven fabric by using an air jet and a collecting net in place of a winder. The nonwoven fabric was obtained by

* Corresponding author.
E-mail address: a-suzuki@yamanashi.ac.jp (A. Suzuki).

0032-3861/$ - see front matter © 2007 Elsevier Ltd. All rights reserved.
doi:10.1016/j.polymer.2007.03.028

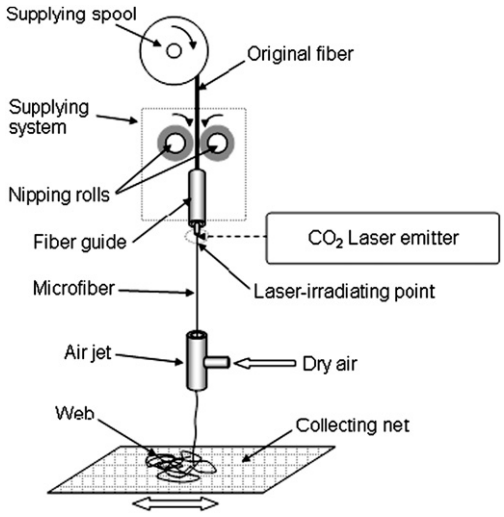

Fig. 1. CO_2 laser-thinning apparatus used for web formation.

this method without using any solvent such as electrospun and flashspun fabrics and composed of endless microfibers with a uniform diameter. The obtained microfiber was slightly oriented along fiber axis by the flow-induced crystallization.

We present here the results pertaining to the PET nonwoven fabric obtained by CO_2 laser-thinning method.

2. Experimental

2.1. Material

The original PET fiber used in the present study was a commercial grade fiber ($\overline{M}_w = 55,000$, $\overline{M}_n = 33,000$) and had a diameter of 143.6 μm, degree of crystallinity of 4.5%, and birefringence of 0.070. The original fiber was almost amorphous and isotropic fiber.

2.2. Measurements

The morphology of microfiber was determined with scanning electron microscopy (SEM) (JSM-6060LV, JEOL Ltd., Japan). SEM micrographs of the fibers were observed with an accelerating voltage of 10 kV. Before the observation, the samples were coated with gold using a sputter coater. The average diameter and the diameter distribution were obtained by using imaging analyzer (SMile View, JEOL Ltd., Japan).

Birefringence was measured with a polarizing microscope equipped with a Berek compensator (Olympus Optical Co., Ltd., Japan).

Wide-angle X-ray diffraction images of the nonwoven fabrics were taken with an imaging-plate (IP) film and an IP detector *R*-AXIS DS3C (Rigaku Co., Akishima, Japan). The IP film was attached to the X-ray generator (Rigaku Co.) operated at 40 kV and 200 mA. The radiation used was Ni-filtered Cu Kα. The sample-to-film distance was 40 mm. The fiber was exposed for 5 min to the X-ray beam from a pinhole collimator with a diameter of 0.4 mm.

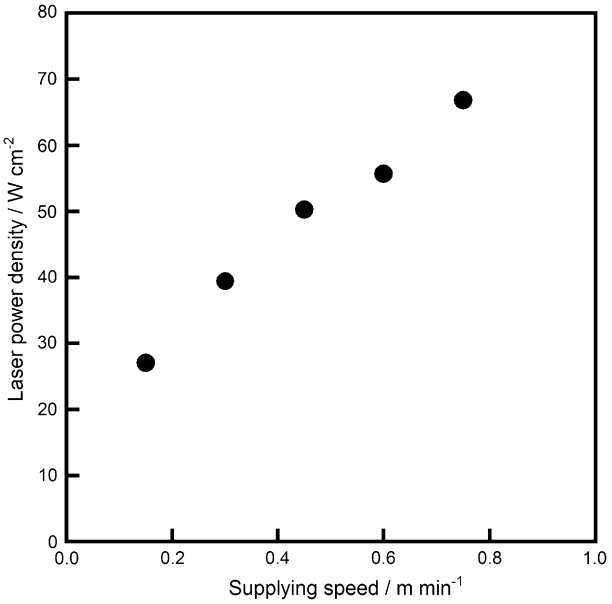

Fig. 2. Relationship between supplying speed and the optimum laser power density to make the microfiber.

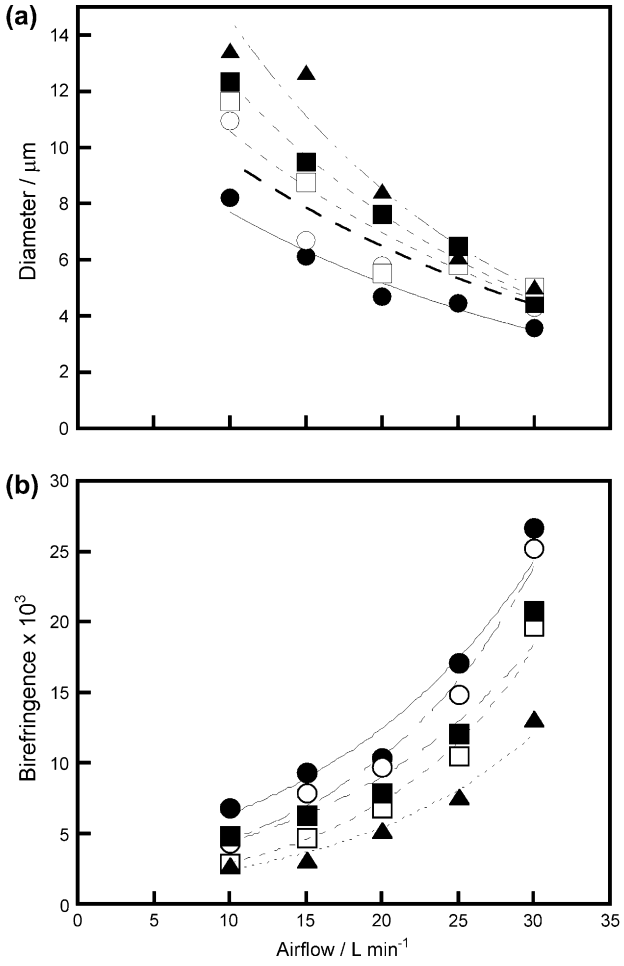

Fig. 3. Airflow dependence of fiber diameter (a) and birefringence (b) of webs obtained various supplying speeds (S_s), ●: $S_s = 0.15$ m min^{-1}, ○: $S_s = 0.30$ m min^{-1}, ■: $S_s = 0.45$ m min^{-1}, □: $S_s = 0.60$ m min^{-1}, ▲: $S_s = 0.75$ m min^{-1}.

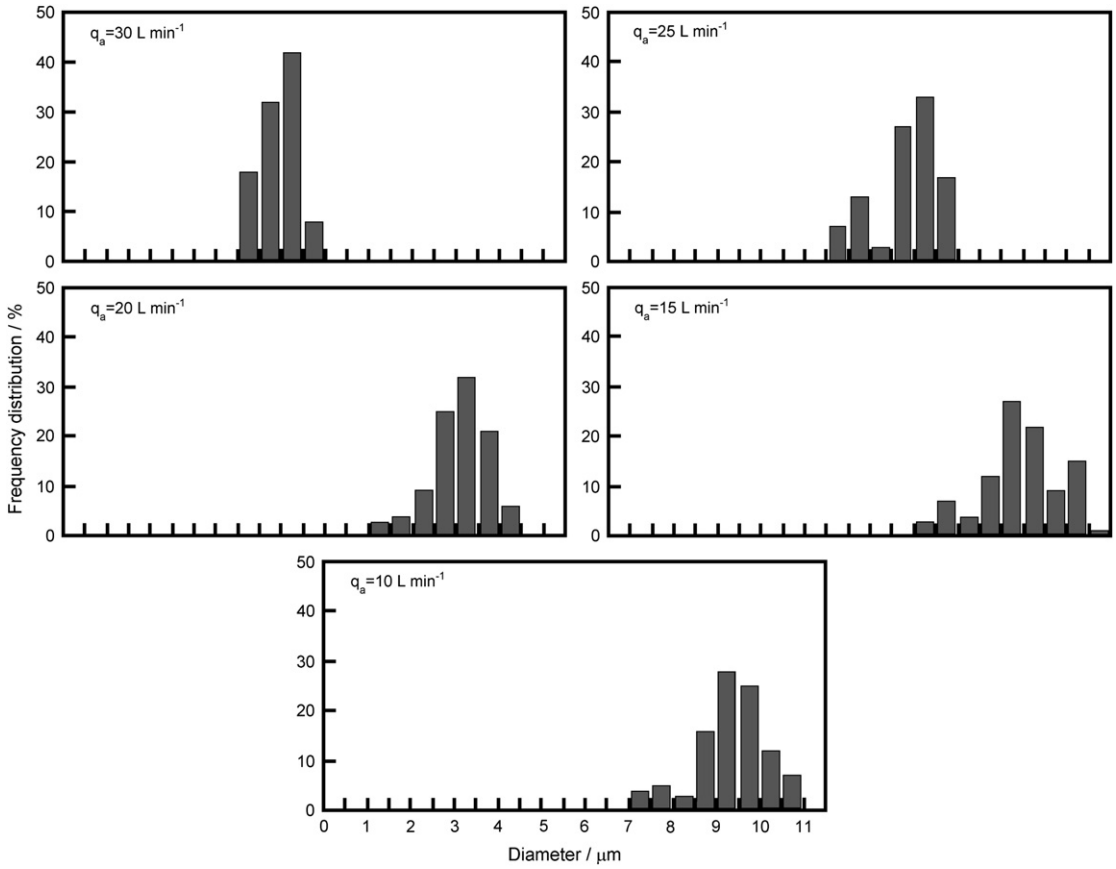

Fig. 4. Fiber diameter distributions of microfibers obtained at five different airflow rates (q_a) (supplying speed: 0.75 m min^{-1}).

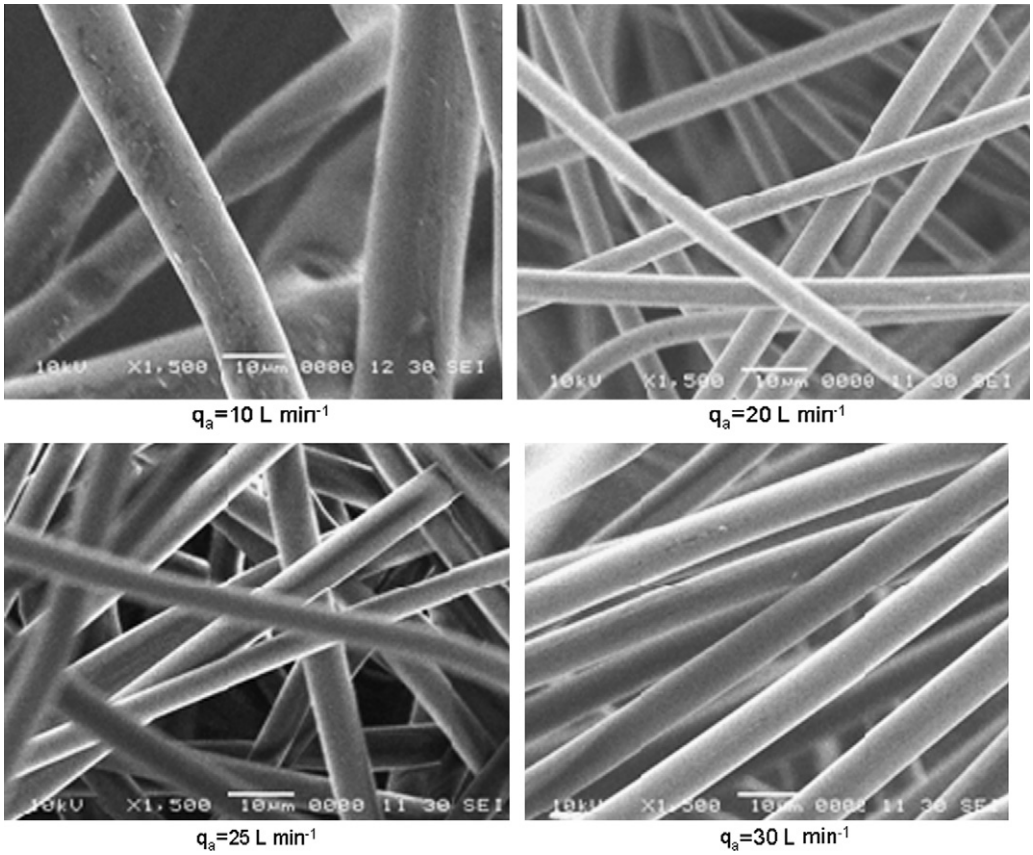

Fig. 5. SEM photographs of 1500 magnifications for the microfibers obtained at four different airflow rates (q_a) (supplying speed: 0.15 m min^{-1}).

The DSC measurements were carried out using a THERM PLUS 2 DSC 8230C calorimeter (Rigaku Co.). The DSC scans were performed within the temperature range of 25–280 °C, using a heating rate of 10 °C min^{-1}. All DSC experiments were carried out under a nitrogen purge. The DSC instrument was calibrated with indium. The degree of crystallinity (X_c) was determined from heat of fusion (ΔH_m) and enthalpy of cold crystallization (ΔH_{cc}) as follows:

$$X_c\,(\%) = [(\Delta H_m + \Delta H_{cc})/-126.6] \times 100$$

where -126.6 J g^{-1} is used as the heat of fusion of the crystalline phase of PET [27].

2.3. CO_2 laser-thinning apparatus used for web formation

The CO_2 laser-thinning apparatus to continuously produce the web consists of supplying motor with spool with a diameter of 90 mm, a continuous wave CO_2 laser emitter, supplying system composed of a fiber guide and nipping rolls, an air jet, and a collecting net as shown in Fig. 1. The continuous wave CO_2 laser emitted at 10.6 μm, and the laser beam was a 2.0 mm diameter spot. The laser power was measured by the power meter during the laser irradiation. The laser power density was estimated by dividing the measured laser power in the area of the laser spot. The laser power of more than 90% is obtained in the area of the laser spot. It is necessary to supply the original fiber to a laser-irradiating point at a constant speed in order to stably obtain the microfiber web with a uniform diameter. The supplying system pulls out the original fiber of the supplying spool and supplies it to the laser-irradiating point at a constant speed. The supplying system plays an important role in the CO_2 laser-thinning apparatus. The fiber attenuated at the laser-irradiating point is pulled out on the collecting net by the air jet, and the webs with a uniform diameter are formed by reciprocating the collecting net at constant speed.

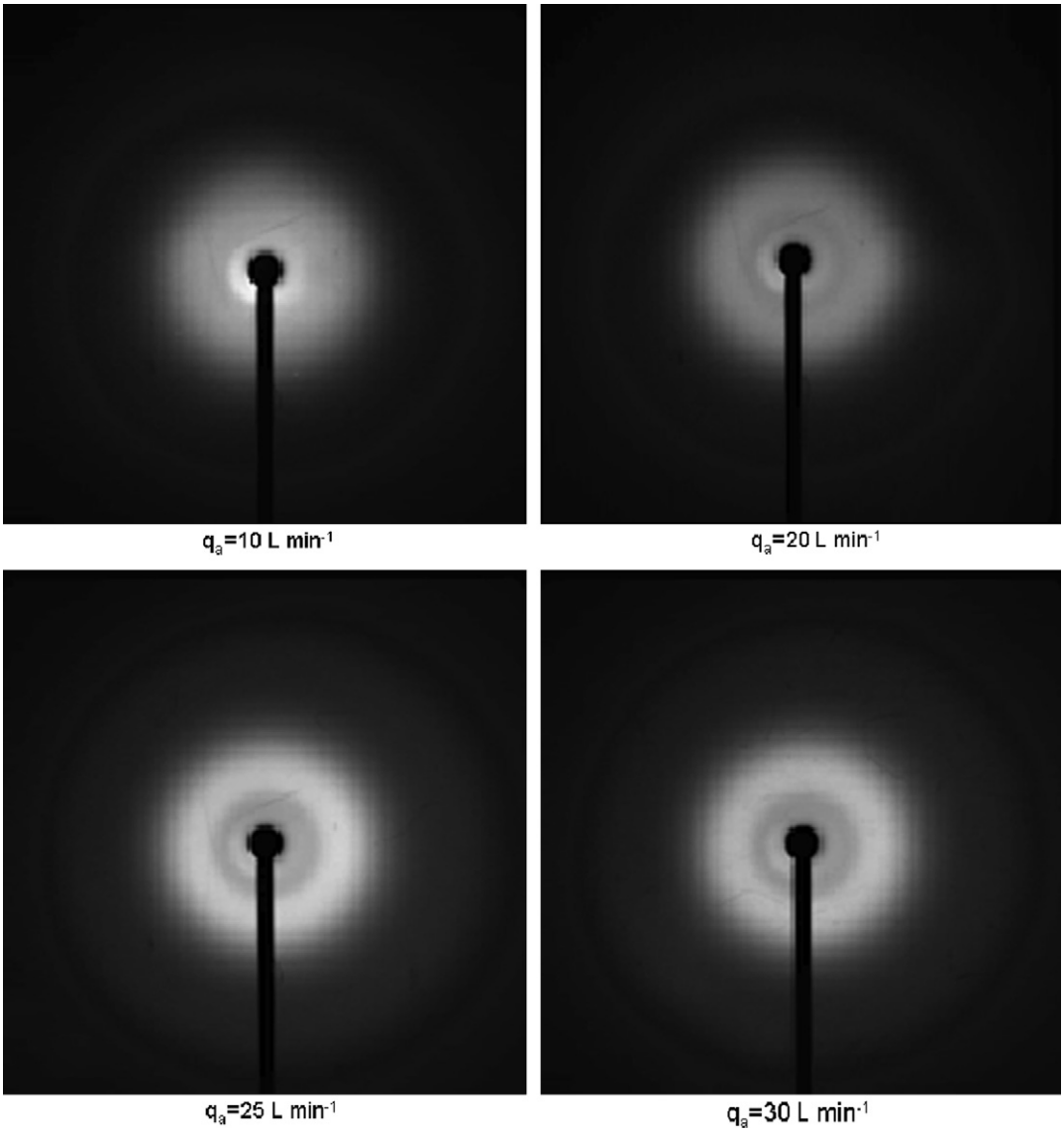

Fig. 6. Wide-angle X-ray diffraction patterns for the microfibers obtained at four different airflow rates (q_a) (supplying speed: 0.15 m min^{-1}).

2.4. Annealing of nonwoven fabrics

To make nonwoven fabrics from the web corrected on the net and to improve its mechanical properties, the web was annealed in a vacuum oven. The four edges of the web were fixed with four clamps, and the fixed web was annealed at different temperatures varying from 130 to 190 °C for various annealing times ranging from 5 to 20 min.

3. Results and discussion

3.1. Web formation

In the web formation by the laser-thinning apparatus, the fiber diameter of the web was determined by the supplying speed, the laser power density, and airflow rate.

Fig. 2 shows the relationship between supplying speed and an optimum laser power density to stably make the microfiber. The laser power density increased linearly as the supplying speed increased and was closely related with the supplying speed. There was optimum laser power density for each supplying speed. Henceforth the laser thinning at each supplying speed was carried out at the optimum laser power density.

Fig. 3(a) and (b) shows the airflow rate dependence of the diameter and the birefringence for the PET webs obtained at five different supplying speeds (S_s). The increase of airflow led to an increase in the air suction speed and drag force. The diameter of the microfiber web obtained at each S_s decreases as the airflow increased. The decrease in throughputs led to an increase in the draw force and then the reduction in fiber diameter. When the fiber prepared by irradiating the laser operated at a power density of 4.8 W cm^{-2} to the original fiber supplied at $S_s = 0.15$ m min^{-1} was dragged at an airflow rate of 30 L min^{-1}, the thinnest microfiber web with a diameter of 3.6 μm was obtained. The fiber diameter decreases with an increase in the air suction speed.

Fig. 3(b) shows the airflow rate dependence of the birefringence for the microfibers obtained at five different supplying speeds (S_s). The birefringence of the microfiber produced at each S_s increased as the airflow rate increased. The highest birefringence of 0.028 was obtained when the fiber, obtained by irradiating the laser to the original fiber supplied at 0.15 m min^{-1}, was dragged at an airflow rate of 30 L min^{-1}. This birefringence was lower than that of the laser-thinned PET microfiber wound up on a spool, previously reported [22]. The microfiber wound at the speed of 2000 m min^{-1} had a birefringence of 0.097 and a diameter of 2.8 μm. The difference in degree of the orientation between the web and the wound microfiber is attributable to the difference in the drawing force between the air suction and the winding.

In general, the total birefringence is the sum of the crystalline and amorphous birefringence values [28], and when the birefringence of PET was ≥0.070, the strain-induced crystallization is assumed to occur [29]. The increase of birefringence with the airflow rate is attributed to the increases in the degree of the molecular chain orientation without a flow-induced crystallization because the web had no reflections due to crystallites. The detailed discussion of crystallization is found later (see Fig. 6).

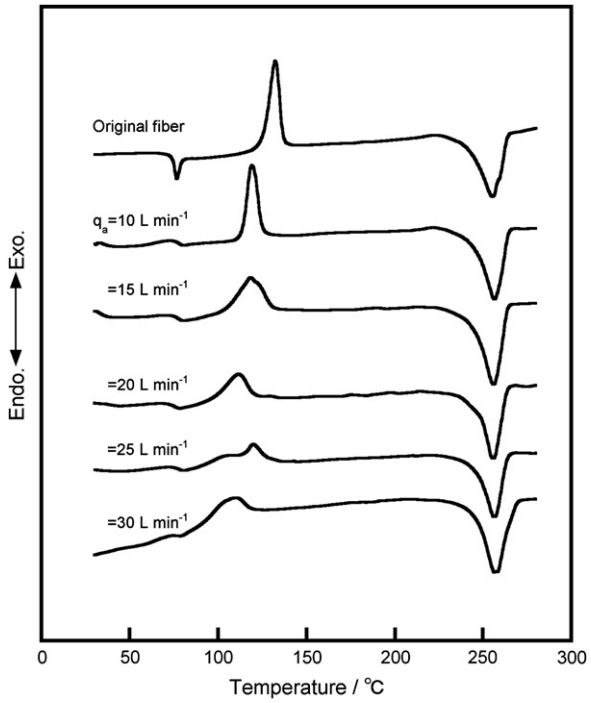

Fig. 7. DSC curves of original fiber and webs at five different airflow rates (q_a).

Fig. 4 shows the distribution of diameters of microfibers obtained at five different airflow rates. As the airflow rate increased, the diameter distribution becomes gradually narrower, and the average fiber diameter decreased. In the web formation carried out at the airflow rate above 30 L min^{-1}, however, the diameter distribution is becoming gradually broader with increasing airflow rate. The uniformity of web decreased and the average fiber diameter increased because the higher airflow rate above 30 L min^{-1} swayed the fiber at laser-irradiation point.

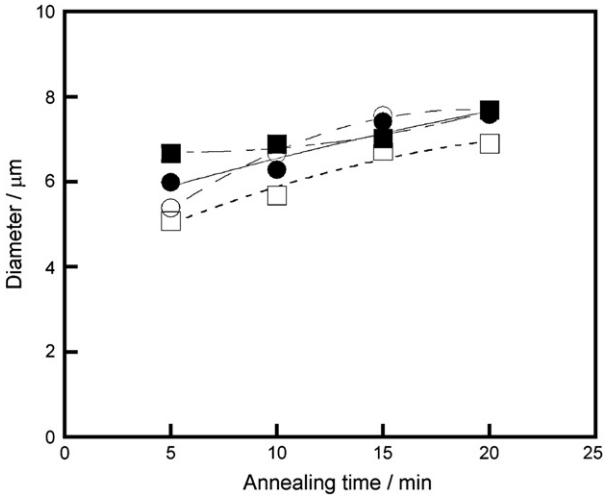

Fig. 8. Annealing time dependence of fiber diameter in the nonwoven fabrics treated at various annealing temperatures (T_{an}) in a vacuum oven. ●: $T_{an} = 190$ °C, ○: $T_{an} = 170$ °C, ■: $T_{an} = 150$ °C, □: $T_{an} = 130$ °C.

Fig. 5 shows the SEM photographs of 1500 magnifications for the webs obtained at four airflow rates. The four webs were obtained by laser-irradiating the original fiber supplied at $S_s = 0.15\ m\ min^{-1}$. The observation by the SEM photographs shows that the webs have a smooth surface without a surface roughened by laser ablation, and there is no droplet in the webs.

Fig. 6 shows that the wide-angle X-ray diffraction (WAXD) patterns of the webs were dragged at four different airflow rates (q_a). The supplying speed was $0.15\ m\ min^{-1}$. The webs have no reflections due to crystallites, and only an amorphous halo was observed. The results show that the flow-induced crystallization did not take place in the web formation processing.

Fig. 7 shows the DSC curves for the original fiber and the webs obtained at various airflow rates (q_a). The original fiber shows a change in slope in the specific heat at 76 °C, which corresponds to the T_g; an exothermic transition at 132 °C caused by a cold crystallization; and a broad melting endotherm peaking at 255 °C. Its melting peak can be ascribed to the lamellar crystals crystallized during the DSC scanning [30,31].

The web obtained at an airflow rate of $30\ L\ min^{-1}$ has a cold crystallization temperature (T_{cc}) of 110 °C and a melting temperature (T_m) of 255 °C. Its T_{cc} is 22 °C lower than that of the original fiber. The decrease in the T_{cc} was caused by the increase in the degree of orientation of amorphous chains.

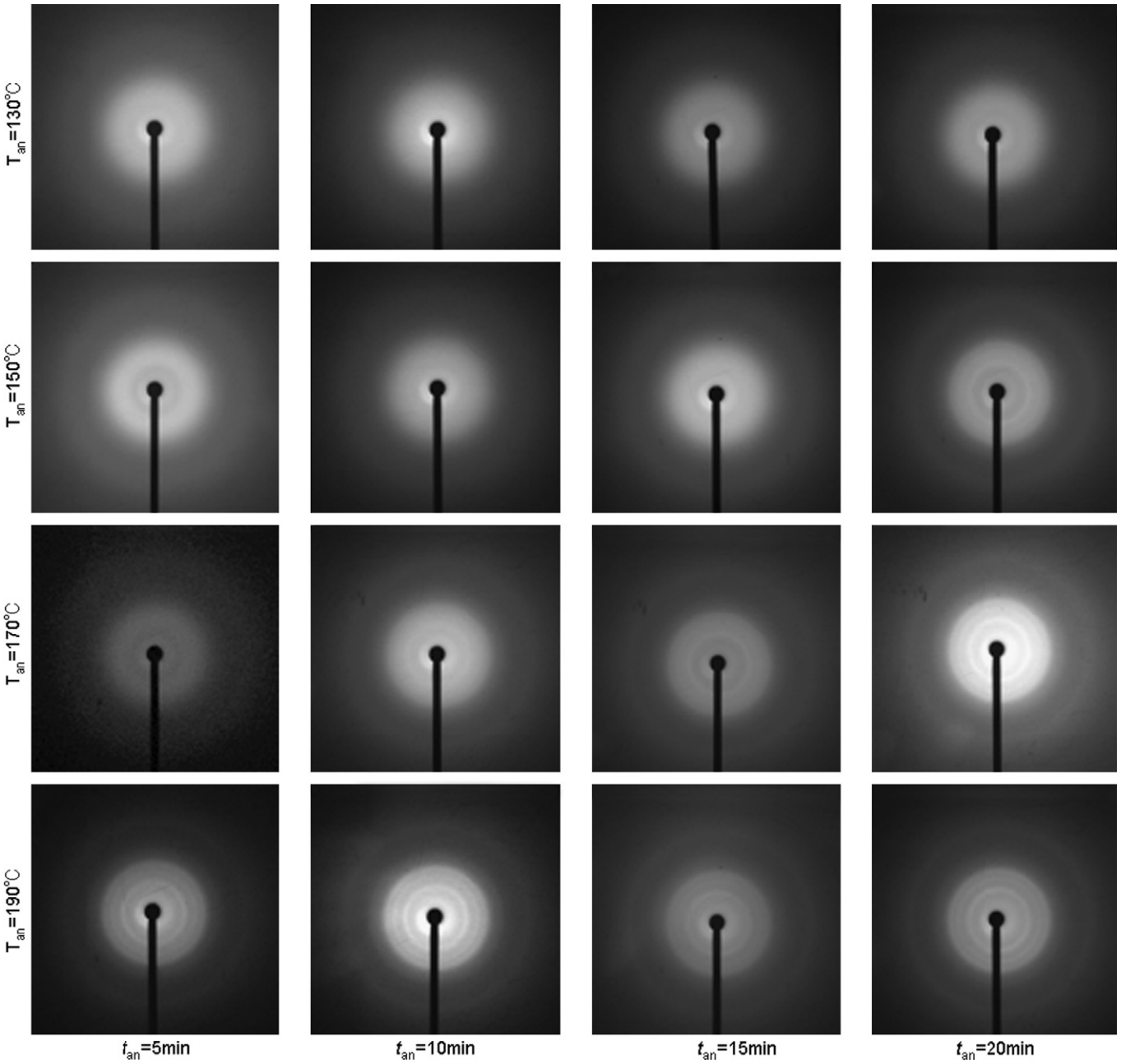

Fig. 9. Wide-angle X-ray diffraction patterns of the nonwoven fabrics annealed under various conditions.

The crystals existed in the web obtained at various airflow rates were ascribed to the lamellar crystals formed during the DSC scanning because their T_ms are the same as that of the original fiber.

3.2. Annealing of web

To make nonwoven fabrics from the microfiber web and to improve its mechanical properties, the web fixed with the clamps was annealed under various annealing conditions. The annealing at fixed length induced the thermal shrinkage of microfibers and led to closer packing of microfiber.

Fig. 8 shows annealing time dependence of fiber diameter in the nonwoven fabrics treated at various annealing temperatures in a vacuum oven. The webs used for the annealing carried out under various conditions were obtained at a supplying speed of 0.75 m min^{-1} and an airflow rate of 30 L min^{-1} and had a diameter of about 5 μm. As the annealing time increased, the diameter increased further and the microfibers annealed for 20 min at the annealing temperatures except 130 °C had a diameter of about 7.5 μm. The annealing at higher temperature induced the larger thermal shrinkage. The larger shrinkage increased further the fiber diameter because the volumes of microfibers before and after the annealing were considered to be approximately constant.

Fig. 9 shows the WAXD patterns of the nonwoven fabrics annealed under various conditions. The nonwoven fabrics annealed at 130 °C do not have reflections due to crystallites, and only an amorphous halo was observed. The intensity of Debye–Scherrer rings due to crystallites increased as the annealing temperature and annealing time increased. The inside ring is attributable to the (010) reflection, and outside rings to ($\bar{1}$10 and 100) reflections. In the nonwoven fabric annealed at 190 °C even for an annealing time of 5 min, the Debye–Scherrer rings were observed.

Fig. 10 shows the DSC curves for nonwoven fabrics annealed at four different annealing temperatures (T_{an}) for 20 min. All the annealed nonwoven fabrics show the cold crystallization temperature (T_{cc}) of 116 °C caused by cold crystallization; and a broad melting endotherm peaking at 256 °C. The exothermic peak due to the cold crystallization decreased as the annealing temperature increased, and that of the nonwoven fabric annealed at 190 °C shows only the trace of the peak. The area of the melting peak increased as the annealing temperature increased. The melting points (T_m) of all the annealed nonwoven fabrics are similar to that of the original fiber. These melting peaks can be ascribed to the lamellar crystals, which crystallized during the annealing and the DSC scanning. Elenga et al. [32] suggested from the standpoint of kinetics that the low-temperature melting peak was ascribed to the fringed-micelle crystals built up by chain unfolding, and the high-temperature one corresponds to the untransformed fraction of the lamellar crystals that undergo reorganization during the heating scan. The fringed-micelle crystals were not existed in the annealed nonwoven fabrics because the melting peak lower than that based on the lamellar crystals cannot be observed in their DSC curves.

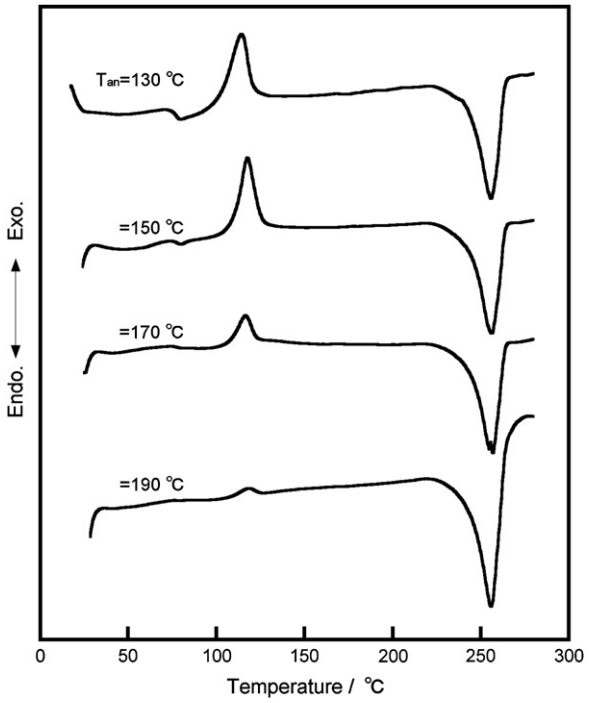

Fig. 10. DSC curves of nonwoven fabrics annealed at four different annealing temperatures (T_{an}) for 20 min.

The decrease in area of the cold crystallization peak and the increase in that of melting peak with increasing the annealing temperature and annealing time mean that the lamellar crystals formed during the annealing increased.

Fig. 11 shows the changes in the degree of crystallinity (X_c), which was estimated from the DSC data of the nonwoven fabrics annealed at the temperature range of 130–190 °C, with annealing time. The X_c value at each annealing time increased

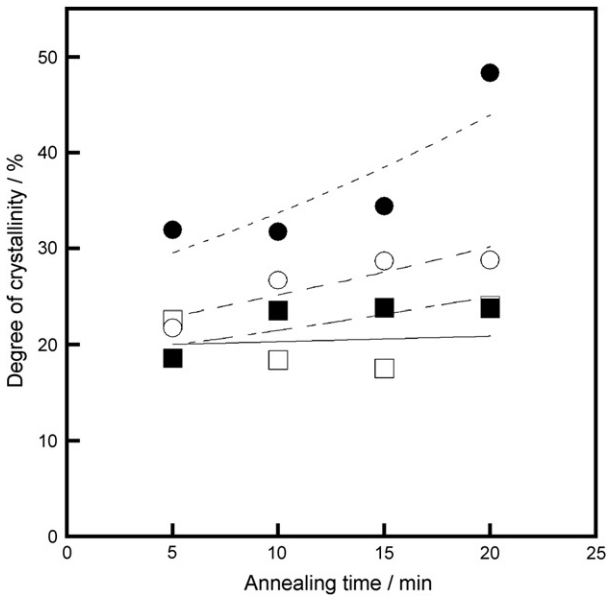

Fig. 11. Changes in the degree of crystallinity (X_c), which was estimated from the DSC data of the nonwoven fabrics annealed at the temperature range of 130–190 °C, with annealing time.

as the annealing temperature increased, and that at each annealing temperature increased with annealing time. The nonwoven fabrics annealed at 190 °C for 20 min had the highest X_c value of 48%.

4. Conclusions

The CO_2 laser-thinning method was applied to the PET fiber to prepare the PET nonwoven fabric without using the solvent. The nonwoven fabric obtained was made of the endless microfibers with a uniform diameter without droplet.

The laser-thinning method was found to be effective in producing other nonwoven fabrics such as poly(L-lactic acid) (PLLA) and poly(glycolic acid) (PGA). The PLLA and PGA nonwoven fabrics prepared by using the laser-thinning method will be reported at a later date.

Acknowledgment

We acknowledge the financial support of the Grant-in-Aid for Scientific Research (B) of Japan Society for the Promotion of Science.

References

[1] Ariawan AB, Hatzikiriakos SG, Goyal SK, Hay H. Adv Polym Technol 2001;20:1.
[2] Zhao R, Wadsworth LC. J Appl Polym Sci 2003;89:1145.
[3] Zhao R, Wadsworth LC. Polym Eng Sci 2003;43:463.
[4] Bhat G, Malkan S. J Appl Polym Sci 2002;83:572.
[5] Nanjundappa R, Bhat GS. J Appl Polym Sci 2005;98:2355.
[6] Bhat GS, Jangala PK, Spruiell JE. J Appl Polym Sci 2004;92:3593.
[7] Dinga B, Kimuraa E, Satoa T, Fujitaa S, Shiratori S. Polymer 2004;45:1895.
[8] Gupta P, Wilkes GL. Polymer 2003;44:6353.
[9] Ayutsede J, Gandhi M, Sukigara S, Micklus M, Chen HE, Ko F. Polymer 2005;46:1625.
[10] Fong H. Polymer 2004;45:2427.
[11] Yeo Y, Jeon D, Kim C, Choi S, Cho K, Lee Y, et al. J Appl Polym Sci 2004;72:86.
[12] Lee K, Givens S, Chase DB, Rabolt JF. Polymer 2006;47:8013.
[13] Zong X, Kim K, Fang D, Ran S, Hsiao BS, Chu B. Polymer 2002;43:4403.
[14] Kumar RN, Hee KC, Rozman HD. J Appl Polym Sci 2005;95:1493.
[15] Meng J, Song L, Meng J, Kong H, Zhu G, Wang C, et al. J Biomed Mater Res 2006;79A:298.
[16] You Y, Min BM, Lee SJ, Lee TS, Park WH. J Appl Polym Sci 2005;95:193.
[17] Kim B-S, Mooney DJ. J Biomed Mater Res 1998;41(2):322–32.
[18] Higgins SP, Solan AK, Niklason LE. J Biomed Mater Res 2003;67A:295.
[19] Jinming G, Niklason L, Langer R. J Biomed Mater Res 1998;42:417.
[20] Eugene DB, Todd AT, David GS, Gary EW, Gary LB. J Biomed Mater Res 2004;71B:144.
[21] Jue Z, Chen FL. Polym Eng Sci 2004;44:331.
[22] Suzuki A, Okano T. J Appl Polym Sci 2004;92:2989.
[23] Suzuki A, Kamata K. J Appl Polym Sci 2004;92:1454.
[24] Suzuki A, Narisue S. J Appl Polym Sci 2006;99:27.
[25] Suzuki A, Hasegawa T. J Appl Polym Sci 2006;99:802.
[26] Suzuki A, Mizuochi D, Hasegawa T. Polymer 2005;46:5550.
[27] Brandrup J, Immergut EH, editors. Polymer handbook. 4th ed. New York: J. Wiley & Sons; 1998. p. VI/42.
[28] Stain RS, Norris FN. J Polym Sci Part A2 2001;82:2775.
[29] Yamada H, Kikutani U, Takaku A, Shimizu J. Sen-i Gakkaishi 1988;44:177.
[30] Pecorini TJ, Hertzberg RW. Polymer 1993;34:5053.
[31] Quintanilla L, Rodriguez-Cabello JC, Pastor JM. Polymer 1994;35:2321.
[32] Elenga R, Seguela R, Rietsch F. Polymer 1991;32:1975.